

Detecting Hallucinations in Large Language Models via Internal Attention Divergence Signals

Gijs van Dijk

Utrecht University

g.vandijk1@students.uu.nl

Abstract

We propose a lightweight and single-pass uncertainty quantification method for detecting hallucinations in Large Language Models. The method uses attention matrices to estimate uncertainty without requiring repeated sampling or external models. Specifically, we measure the Kullback–Leibler divergence between each attention head’s distribution and a uniform reference distribution, and use these features in a logistic regression probe. Across multiple datasets, task types, and model families, attention divergence is highly predictive of answer correctness and performs competitively with existing uncertainty estimation methods. We find that this signal is concentrated in middle layers and on factual tokens such as named entities and numbers, suggesting that attention dynamics provides an efficient and interpretable white-box signal of model uncertainty.

1 Introduction

LLMs achieve strong performance across tasks such as question answering, summarization, and reasoning (Zhao et al., 2023). Despite these advances, LLMs are known to generate incorrect or unsupported content, often referred to as hallucinations (Kalai et al., 2025), which makes them less reliable in situations where factuality is important. An issue with addressing this problem is that model outputs typically do not reflect the model’s own uncertainty. Autoregressive language models are trained to generate fluent continuations, which can result in overconfident falsehoods. As a result, users cannot reliably distinguish between correct and incorrect outputs.

Hallucinations pose large risks in high-stakes areas such as healthcare (Kim et al., 2025), law (Magesh et al., 2024). Prior work has emphasized the need to detect and mitigate hallucinations, particularly in settings requiring factual reliability (Huang et al., 2024). Existing methods often con-

flate fluency with correctness or require substantial computational overhead (Liu et al., 2025).

We propose a simple, single-pass uncertainty measure derived from attention distributions. We compute the Kullback–Leibler (KL) divergence between each attention head’s distribution and a uniform reference distribution representing maximum uncertainty. Intuitively, reliable knowledge may correspond to concentrated attention on informative context tokens, whereas epistemic uncertainty may manifest as diffuse or misallocated attention. We aggregate these divergence signals across heads and layers and use a lightweight lasso-regularized probe to predict answer correctness. The probe serves only to aggregate signals across attention heads; the underlying uncertainty signal originates from the attention divergence itself.

Across multiple datasets, task types, and model families, attention divergence is highly predictive of answer correctness and performs competitively with existing uncertainty estimation methods. We find that the signal is concentrated in middle layers and peaks at factual tokens such as named entities and numbers, suggesting that internal attention dynamics provide an efficient white-box signal of model uncertainty.

2 Background

Recent work suggests that hallucinations in Large Language Models (LLMs) are not merely decoding errors, but arise from properties of the transformer architecture (Vaswani et al., 2017) and its learned internal representations (Huang et al., 2024; Orgad et al., 2024)

Uncertainty can be separated into aleatoric and epistemic uncertainty (Kiureghian and Ditlevsen, 2009; Hüllermeier et al., 2021). In the context of natural language modelling, aleatoric uncertainty is often associated with ambiguous prompts, underspecified questions, or multiple equally valid

continuations (Hou et al., 2023; Ling et al., 2024). This type of uncertainty is inherent to the input and cannot be reduced even with more training data.

Epistemic uncertainty, in contrast, captures uncertainty due to limited knowledge of the model, finite training data, model misspecification, or gaps in learned representations. Unlike aleatoric uncertainty, epistemic uncertainty is, in principle, reducible. This distinction is particularly important for hallucination detection in LLMs. Hallucinations characterized by untruthful outputs are not primarily driven by aleatoric uncertainty, as they typically do not arise from ambiguous prompts. Instead, they reflect epistemic failures where the model produces fluent output despite lacking reliable knowledge (Huang et al., 2024). In such cases, the model appears confident even when its internal knowledge is insufficient.

Uncertainty quantification provides a framework for addressing hallucinations in Large Language Models. Most existing approaches operate in the output space, estimating uncertainty based on the generated text or its associated probabilities. Common methods rely on logit- and likelihood-based signals such as log-likelihood, perplexity, maximum token probability, or predictive entropy (Liu et al., 2025). These approaches assume that low-probability generations correspond to higher uncertainty.

However, this assumption does not hold. Hallucinated statements can receive high likelihood under the model distribution, as autoregressive language models are trained to generate fluent continuations rather than calibrated confidence estimates. As a result, output-based uncertainty signals can fail to distinguish confident errors from reliable knowledge.

This motivates a shift toward internal signals. If hallucinations may arise from failures in internal computation, then signals extracted from hidden states, attention patterns, or other latent representations may provide more reliable indicators of epistemic uncertainty. In this work, we focus on attention as a structured internal probability distribution that may encode such signals.

3 Related Work

A growing body of research has investigated hallucination detection and uncertainty quantification using internal model signals rather than only output probabilities.

3.1 Hidden State Probing

Orgad et al. (2024) show that internal representations encode signals of truthfulness concentrated on answer tokens. Similarly, Binkowski et al. (2025) and Chen et al. (2024) train probes over hidden states to detect hallucinations. However, these approaches often struggle to generalize across tasks and datasets. Probes trained on hidden states tend to capture task-specific correlations rather than a global confidence signal.

3.2 Attention-based Methods

Several recent studies have explored methods that use attention to infer uncertainty signals. Li et al. (2025) introduce Uncertainty Quantification with Attention Chain (UQAC), a white-box method that uses attention weights to identify which reasoning tokens are most influential for producing the answer. Similarly, TOHA (Topology-based Hallucination detector) (Bazarova et al., 2025) analyses topological properties of attention matrices to estimate uncertainty.

In the supervised setting, methods such as Lookback Lens (Chuang et al., 2024) and Attention-Pooling Probes (CH-Wang et al., 2024) train lightweight classifiers over attention-derived features. Lookback Lens uses per-head ratios of attention to context versus generated tokens, while Attention-Pooling Probes pool attention weights across heads and layers. Our method instead uses a KL-divergence-based attention measure with a lightweight probe, relying on low-dimensional, interpretable features.

Other work shows that hallucinations might arise in specific attention heads. Vazhentsev et al. (2025) propose an attention-based uncertainty estimation approach by identifying a subset of uncertainty-aware attention heads whose behaviour changes at hallucinated tokens. Stolfo et al. (2024) similarly report certainty related signals localized in particular neurons.

3.3 Sampling- and Output-Based Methods

A large class of approaches estimates uncertainty directly from model outputs. Sampling-based methods measure disagreement across multiple generations, such as semantic entropy (Farquhar et al., 2024) or SelfCheckGPT (Manakul et al., 2023). Other methods rely on output probabilities, perplexity, or entropy (Ren et al., 2022; Liu et al., 2025). Some approaches use external verifiers or

ensembles (Kuhn et al., 2023).

While often effective, these methods typically require repeated sampling or additional models. In contrast, our method operates in a single forward pass and extracts uncertainty signals directly from attention distributions.

4 Methodology

4.1 Kullback–Leibler Divergence

To create a quantitative signal from attention, we measure how much the attention distribution deviates from a uniform baseline (\mathcal{U}) using Kullback–Leibler (KL) divergence.

It is often useful to quantify how well one probability distribution approximates another. We therefore use the Kullback–Leibler (KL) divergence, which measures the discrepancy between two distributions. Given a reference distribution P and an alternative distribution Q , the KL divergence is defined as the expected log-ratio between P and Q under P .

In our setting, attention weights define a discrete probability distribution over token positions $x \in \{1, \dots, T\}$. The KL divergence therefore takes the form

$$D_{\text{KL}}(P \parallel Q) = \mathbb{E}_{x \sim P} \left[\log \frac{P(x)}{Q(x)} \right]. \quad (1)$$

Intuitively, this quantifies how much extra information (nats¹) is required, on average, when outcomes drawn from distribution P are interpreted as if they were drawn from Q .

When the reference distribution Q is uniform (we will denote this as \mathcal{U} for clarity), the KL divergence simplifies to

$$\sum_x P(x) \log \frac{P(x)}{1/T} = \log T - H(P) \quad (2)$$

where T denotes the number of tokens in the attention context window, so that $\mathcal{U}(x) = 1/T$ assigns equal probability to each context token position.

A higher concentration of attention reflects stronger model confidence, not necessarily correctness. In our hypothesis, hallucinations arise when the model exhibits wrongly calibrated confidence, characterized by highly concentrated attention on

¹Nats denote information measured using natural logarithms (base e).

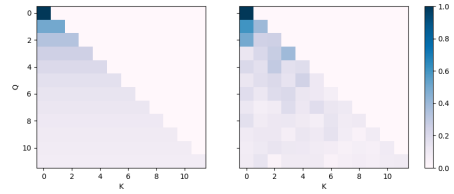


Figure 1: Intuition of attention patterns with low KL divergence to uniform (left) and higher KL divergence to uniform (right). Higher divergence corresponds to more concentrated attention.

misleading tokens. In contrast, near uniform attention distributions are more likely to occur at positions where the model lacks reliable knowledge and remains uncertain, since the model does not know to which token to attend.

4.2 Attention Divergence

In autoregressive transformer models, such as GPT, (Vaswani et al., 2017) the attention weights produced by a single attention head at a given generation step form a discrete probability distribution over the available context tokens. Let $A_t^{(l,h)}$ denote the attention distribution of head h in layer l at generation step t , defined over the t previously generated tokens. We compare this distribution to a uniform reference distribution \mathcal{U} , which assigns equal probability to all context positions and represents a state of maximal uncertainty.

We quantify the separation between these two distributions using KL divergence. This measures how much an attention head focuses on a subset of previous tokens. For each attention head, the KL divergence is computed at every generation step and averaged across the generation answer tokens, yielding a single scalar feature per head. These per-head divergence values form a feature vector that summarizes the attention during generation.

Formally, for each example we construct a feature vector $x_i \in \mathbb{R}^{L \times H}$ where each entry corresponds to the mean KL divergence of a single attention head pooled over the generated answer tokens.

4.3 Probing

To predict answer correctness and uncertainty from the attention divergence features, we train a logistic regression probe with lasso (L1) regularization. The model estimates $P(y_i = 1 \mid x_i) = \sigma(w^\top x_i + b)$, where σ is the logistic sigmoid function, and $w \in \mathbb{R}^{L \times H}$ is the weight vector.

We train a logistic regression probe with L1

(lasso) regularization by minimizing

$$\mathcal{L}(w, b) = - \sum_{i=1}^N [y_i \log p_i + (1 - y_i) \log(1 - p_i)] + \lambda \|w\|_1 \quad (3)$$

where $p_i = \sigma(w^\top x_i + b)$, and λ controls the strength of the sparsity penalty. We use lasso (L1) regularization to select a sparse subset of attention heads that the probe thinks are the most predictive of correctness. This provides insight into where these heads are located.

We use stratified k-fold cross-validation to assess stability. We report AUROC as the main metric, which is insensitive to class imbalance (Li, 2024) and captures the quality of probabilistic ranking. We treat correct answers as the positive class ($y = 1$). For each example i , the probe outputs a score $p_i = P(y_i = 1 | x_i)$ where x_i denotes our attention divergence feature on the i -th generated answer, and $y_i \in \{0, 1\}$ classifies whether that answer is correct. We compute AUROC over all examples (both correct and incorrect) by varying a threshold on p_i and measuring the resulting true-positive and false-positive rates. Under this definition AUROC corresponds to the probability that a randomly chosen correct answer is assigned a higher score than a randomly chosen incorrect answer.

We additionally report the Expected Calibration Error (ECE) to see how well our probe is calibrated (Pavlovic, 2025; Wang, 2023). In addition, we measure accuracy. Although accuracy is not a reliable metric for class imbalance (Kubat and Matwin, 1997), we still report it, as it provides additional context along AUC and ECE. To assess stability, experiments are repeated across multiple random dataset shuffles.

5 Experiments

5.1 Configuration

For our main evaluation we use three different instruction tuned models: Llama-3.2-3B-Instruct (Grattafiori et al., 2024), Qwen3-4B-Instruct (Yang et al., 2025), and Mistral-7B-Instruct-v0.2 (Jiang et al., 2023). Models with instruction tuning create more structured outputs without requiring much prompt engineering (Zhang et al., 2023).

We evaluate our method on 4 different datasets spanning multiple task categories. TriviaQA (Joshi et al., 2017) (open-domain) and TruthfulQA (Lin

Dataset	Model	AUROC
TruthfulQA	Llama-3.2-3B	0.906 ± 0.024
	Qwen3-4B	0.906 ± 0.025
	Mistral-7B	0.891 ± 0.024
TriviaQA	Llama-3.2-3B	0.835 ± 0.004
	Qwen3-4B	0.846 ± 0.001
	Mistral-7B	0.835 ± 0.004
HotpotQA	Llama-3.2-3B	0.8035 ± 0.0219
	Qwen3-4B	0.7963 ± 0.0217
	Mistral-7B	0.7782 ± 0.0061
GSM8K	Llama-3.2-3B	0.7672 ± 0.0305
	Qwen3-4B	0.9450 ± 0.0151
	Mistral-7B	0.7889 ± 0.0270

Table 1: Validation results after training a lasso-regularized probe to predict correctness from attention divergence mean pooled across the generation. Within each dataset, the highest AUROC is shown in bold. Results are reported as mean ± standard deviation over three random seeds and five stratified cross-validation folds.

et al., 2021) (multiple-choice) for factual question answering, HotpotQA (Yang et al., 2018) for multi-hop reasoning question answering, and GSM8K (Cobbe et al., 2021) for mathematical reasoning. For each dataset, we sample data points from 3 different seeds, and use stratified k-fold cross-validation within sample. Answer correctness is computed using task-specific evaluation rules. For TriviaQA, TruthfulQA, and HotpotQA, answers are marked correct based on string matching against gold references. For GSM8K, correctness is computed by extracting and comparing the final numeric answer from the raw generated output. Full experimental details, including exact sample counts per dataset and per seed, are provided in the appendix.

5.2 Results

Table 1 summarizes the performance of the attention divergence signal across different datasets and models. The full results can be found in the appendix table 7 which includes accuracy and Expected Calibration Error (ECE).

Attention divergence is predictive of answer correctness across a range of tasks and model families. On factual questioning (QA) benchmarks (TruthfulQA and TriviaQA), performance is particularly strong. Across all three models, AUROC values exceed 0.89 on TruthfulQA and 0.83 on TriviaQA, with relatively small variance across seeds and folds. This suggests that our measure is stable

Method	Single Gen.	Mistral-7B
Ours	Y	0.78 ± 0.02
TOHA [1]	Y	0.71 ± 0.08
SelfCheckGPT [29]	N	0.70 ± 0.06
Semantic entropy [10]	N	0.70 ± 0.05
EigenScore [4]	N	0.68 ± 0.04
HaloScope [7]	Y	0.60 ± 0.06
LLM-Check [34]	Y	0.48 ± 0.03
Perplexity [33]	Y	0.55 ± 0.06
Max entropy [9]	Y	0.62 ± 0.04
ReDEEP [36]	Y	0.49 ± 0.04

Table 2: AUROC on the HotpotQA dataset using Mistral-7B. Baseline results are taken from Bazarova et al. (2025). Our method is evaluated under the same model and dataset.

for detecting incorrect or hallucinated answers. Despite accuracy not being the most reliable metric in situations with high class imbalance (Kubat and Matwin, 1997), it has similar results, with values generally above 0.80 for TruthfulQA and close to or above 0.77 on TriviaQA. The ECE remains moderate on TruthfulQA, which comes partly due to the smaller sample size of just 216 samples across 3 seeds. The ECE is notably low on TriviaQA, indicating that the probe is reasonably well calibrated.

For multi-hop reasoning on HotpotQA, performance is slightly lower. AUROC values range from 0.78 to 0.80. Accuracy remains in the 0.70 range, and calibration is comparable to TriviaQA, with most ECE values below 0.10.

On mathematical reasoning (GSM8K), performance varies more strongly. Qwen3-4B-Instruct achieves high AUROC and accuracy, whereas Llama and Mistral show more moderate results. Despite this variability, AUROC values remain well above chance for all models. In a binary setting, an AUROC of 0.5 corresponds to random ranking, i.e., the model assigns higher scores to correct than incorrect answers only half the time on average. Even in generation tasks with many steps, the method still provides an uncertainty signal. Calibration on GSM8K is also good, with low ECE values (0.04-0.06) across all models.

5.2.1 Comparison to Prior Work

We compared our method to existing uncertainty quantification and hallucination detection methods in settings where direct comparison is possible. Table 2 reports results on the HotpotQA (Yang et al., 2018) dataset using the Mistral-7B model (Jiang et al., 2023). In this setting, our

Method	TriviaQA	TruthfulQA
Ours	0.835	0.906
LapEigvals [2]	<u>0.836</u>	<u>0.829</u>
Hidden States (probe) [2]	0.850	0.823

Table 3: AUROC on TriviaQA and TruthfulQA using Llama-3.2-3B. The highest AUROC value is boldfaced, the runner-up is underlined.

method achieves an AUROC of 0.78 ± 0.02 , outperforming both sampling-/ensemble-based methods and other single generation baselines reported by (Bazarova et al., 2025). Our method also improves over TOHA (Topology-based Hallucination detector) (Bazarova et al., 2025), which is also attention-based and relies on topological features of attention matrices. Compared to output-based uncertainty measures, such as semantic entropy (Farquhar et al., 2024), SelfCheckGPT (Manakul et al., 2023), and other baselines (Ren et al., 2022; Sun et al., 2024; Fadeeva et al., 2024; Sriramanan et al., 2024; Du et al., 2024; Chen et al., 2024), our method provides a stronger AUROC signal, while requiring only a single forward pass.

Table 3 compares our results to Binkowski et al. (2025) on TriviaQA and TruthfulQA. Our method achieves competitive performance on TriviaQA and improves AUROC on TruthfulQA. Across both comparisons, our method consistently performs well, all while requiring less computation. These results support the claim that local attention dynamics encode meaningful uncertainty information and can be used for hallucination detection.

5.3 Sanity Checks

To verify that our proposed signal is not caused by possible other factors, we evaluate a set of sanity checks on TriviaQA using the Llama-3.2-3B-Instruct model. These baselines include simple properties of the generated output and prompt that could possibly correlate to answer correctness. Specifically, we measure: generation length, prompt length, raw output length, final token punctuation, and the amount of digits in the output. We calculate AUROC for all these baselines.

Each baseline is evaluated independently by computing its AUROC with respect to answer correctness. All sanity checks achieve AUROC values close to chance or exhibit weak reverse correlations with correctness.

Additionally, we compute AUROC after permut-

Ablation	AUROC
Remove top-5 heads	0.857 ↓
Remove top-10 heads	0.853 ↓
Remove top-20 heads	0.862 ↑
Remove top-50 heads	0.872 ↑
Remove early layers	0.849 ↓
Remove middle layers	0.844 ↓
Remove late layers	0.862 ↑
Max pooling	0.795 ↓

Table 4: Ablation results on TriviaQA using Llama-3.2-3B. Without ablations the result was an AUROC of 0.858. Increases in AUROC are annotated with ↑, decreases by ↓

ing the correctness labels. Because permutation destroys any true relationship between the features and the labels, we show that the measured signals are not caused by any leakage (such as the labels being known beforehand). These sanity check results show that our main results are not caused by any of these baselines.

The table for sanity checks can be found in the appendix.

5.4 Ablation Experiments

To better understand our measure we perform a series of ablation experiments on the TriviaQA dataset. The results are shown in Table 4.

First, we ablate the most influential attention heads that were identified by the L1-regularization probe by removing the top- k heads ranked by absolute coefficient magnitude. Removing up to $k = 50$ heads does not cause a drop in AUROC relative to the baseline on TriviaQA on Llama-3.2- 3B, it even slightly improves AUROC for some k values. This indicates that the uncertainty signal is not per se localized to a small subset of heads, but is instead encoded across multiple correlated heads.

Next, we ablate entire groups of layers by removing early, middle, or late layers from the feature set. Removing early and middle layers leads to a reduction in AUROC, with the largest drop observed when removing middle layers. This suggests that the signal primarily depends on early-to-middle layers.

We also replaced mean pooling with max pooling. This resulted in a significant performance drop, indicating that the signal is not driven by a small subset of single attention spikes, but by consistent attention diffusion.

Additionally, we perform an ablation experiment where our feature is computed over three different

subsets of the sequence. Specifically, we compute the signal over just the prompt tokens before any tokens are generated, the answer-only, where it is pooled over just the generated token, and the full prompt and answer combination. For solely the prompt tokens we achieve an AUROC of 0.7674, for the answer 0.8707, and for the full generation 0.8215.

Since the prompt only condition is far above chance, a proportion of the uncertainty signal is already present before the model begins to generate tokens. This supports the idea that uncertainty can also be aleatoric, i.e., related to ambiguous prompts or lacking context. This suggests that hallucinations are not solely the result of failures during output generation, but partially due to the prompt itself.

The answer only condition yielded the strongest result, with an AUROC of 0.87.

5.5 Layer & Head Analysis

To investigate whether our proposed attention divergence measure is localized to a specific subset of layers and heads, we analyse the difference in mean attention divergence between correct and incorrect generations. We do this by plotting a heatmap with heads on the x-axis and layers on the y-axis.

Figure 2 visualizes

$$\Delta D_{\text{KL}}(P \parallel \mathcal{U}) = \mathbb{E}[D_{\text{KL}} \mid \text{Correct}] - \mathbb{E}[D_{\text{KL}} \mid \text{Incorrect}] \quad (4)$$

The strongest differences are concentrated in the middle layers of the model. This pattern suggests that our attention divergence measure is not uniformly distributed. Instead, it peaks at the middle layers and is distributed across multiple heads, rather than being dominated by a small subset of attention heads. This explains why removing individual heads has limited effect on overall performance.

We found that attention divergence differs between correct and incorrect generations. To better understand how extreme this difference is, we analyse the distributions using empirical cumulative distribution functions (ECDFs). This allows us to examine how the two groups differ across the entire distribution, with the tails in particular.

For each generated answer, we compute the p -th percentile of the KL divergence between the attention distribution and a uniform baseline. The values

for p that we use are $p \in \{90, 95, 99\}$. The top section of Figure 3 shows the ECDFs for $P(KL \geq x)$, for correct and incorrect answers at each percentile level p . Solid lines correspond to correct generations, whereas dashed lines are incorrect generations.

Across all percentile levels p , incorrect generations exhibit a rightward shift relative to correct generations, indicating more of a right tail in attention divergence. This separation increases along p , showing that the difference between correct and incorrect answers is primarily driven by extreme attention events rather than typical behaviour.

The bottom part of the figure plots the survival ECDFs for correct and incorrect generations and $p = 99$. At each threshold x , the difference measures how much more or less likely correct generations are to exceed x compared to incorrect generations. Negative values indicate that incorrect generations are more likely to exhibit extreme attention divergence. The darker areas around the line indicate the confidence intervals.

Because the difference lies in the extremes and our method is probe dependent it is not possible to give a concrete example comparing the scores of a single truthful to a single false answer generation.

These results do not yet clarify where this uncertainty arises in the generated output. We analyse attention divergence at word level. Since transformers operate on subword units, we aggregate divergence values per word. Each word is then assigned to one of five semantic classes: named entities, numbers, stop words, punctuation, and any other words.

Across the dataset, named entities exhibit higher average attention divergence than generic content words, while stop words and punctuation show lower divergence values. Although numeric tokens occur relatively infrequently, they display high divergence when they do appear. This is likely due to the nature of question answering datasets, which often require recalling specific years or quantities.

This distinction becomes substantially clearer when focusing on extreme divergence events. We compute the 99th percentile of the full word distribution and assign all words whose divergence exceeds this threshold as belonging to the extreme tail. On the TriviaQA dataset, this analysis is based on 1445 generated words, of which 961 are classified as named entities, 435 as other content words, 33 as stop words, and 5 as numeric tokens. About 73% of the words in the 99th percentile tail are

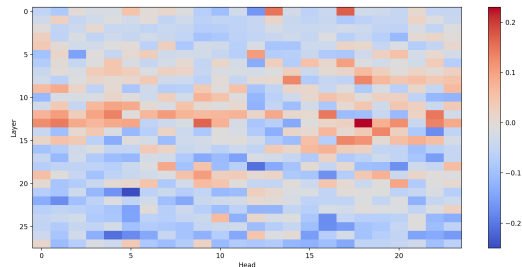


Figure 2: Heatmap of the difference in mean attention divergence between correct and incorrect generations, computed per layer and attention head. Positive values (red) indicate higher divergence for correct answers.

named entities, while the remaining 27% belongs to the "other" distribution. Stop words and punctuation are not in the tail. This indicates that our divergence signal is mostly localized at factual tokens.

The most important observation is that there is cross dataset overlap and generalization. Given the total amount of heads in each model, this represents a small fraction ($\approx 0.5\%$) of the total. Indicating that the signal is not concentrated in a single universal "hallucination-" or "uncertainty-" aware attention head. This result is consistent with earlier findings in literature suggesting that attention heads tend to specialize (Zheng et al., 2024). Other research by Elhage et al. (2021) shows that even when individual heads have specialized roles, meaningful behaviour emerges from how multiple heads interact through the residual stream, instead of a single head. We observed a similar effect, while a few heads reoccur across datasets, most of our proposed signal comes from a larger set of spread out heads.

Although there is overlap across datasets, this does not imply sufficiency. No head appears across all four datasets, and many heads that are highly predictive in the lasso regularized probe are entirely absent in others.

We have also compared the attention heads selected by the probe across all three model families. We consider an attention head to overlap across models if the exact layer \times head pair is selected by the probe in at least one dataset for each model. We find that these overlaps are rare, and that only a small number of pairs occur across two different model families. No single attention head is shared across all three models. For example, a small number of heads overlap between Llama and Qwen, between Llama and Mistral, and between Qwen

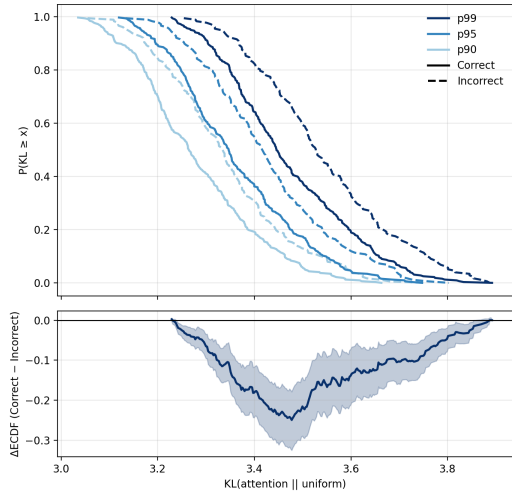


Figure 3: Empirical cumulative distribution functions (ECDFs) of attention divergence values for correct and incorrect generations. Top figure are survival ECDFs $P(KL \geq x)$ computed at the $p \in \{90, 95, 99\}$ percentiles of the token-level KL divergence between attention distributions and a uniform baseline. Solid lines correspond to correct generations, dashed lines are incorrect generations. Bottom figure is the difference between the survival ECDFs for correct and incorrect generations at $p = 99$, with shaded areas indicating confidence intervals (CI).

Model	Early	Middle	Late
Llama-3.2-3B	15.5	53.5	31.0
Qwen3-4B	28.1	35.9	35.9
Mistral-7B	33.8	46.3	20.0

Table 5: Percentage of attention heads selected by the L1 probe (pooled across datasets) located in early, middle, and late layers. Layers are divided into equal thirds by depth.

and Mistral. The complete data is in the appendix.

6 Discussion

Our research investigates whether internal attention mechanisms in LLMs contain reliable signals of epistemic uncertainty, and whether these can be used for hallucination detection. Our results across multiple datasets, models, and ablation experiments provide evidence that attention divergence is predictive of answer correctness.

Our main finding is that attention divergence between attention maps and a uniform reference tends to be higher for incorrect or hallucinated outputs, particularly in the extreme tail of the distribution. This supports the hypothesis that hallucinations also arise from failures in internal computation.

Our ablation experiments provide insight into why this signal works. Removing individual attention heads that were identified by the probe has limited impact on performance. Removing entire groups of layers leads to a degradation in performance, specifically for the middle layers. This indicates there is a sparse subset of attention heads with an unclear relationship that are predictive of answer correctness.

Furthermore, the signal is concentrated on more semantically meaningful tokens, specifically, named entities and numerical values. Stop words and punctuation exhibit low divergence. This pattern matches recent literature showing that hallucination behaviour is related to factual content, rather than randomness. Ferrando et al. (2024) demonstrates that representations tied to entity knowledge are associated with whether a model correctly recalls facts. Likewise, Ogasa and Arase (2025) highlights that failures in processing factual tokens such as numbers or entities can lead to breakdowns in reasoning, whereas this does not happen as much on generic tokens.

A portion of the uncertainty signal is already present within the prompt. When attention divergence is computed solely over the prompt tokens, it remains predictive of answer correctness, even though the performance is weaker than over all answer tokens.

7 Conclusion

We proposed a simple, single-pass uncertainty measure based on the (KL) Divergence between attention matrices and a uniform reference distribution representing maximum uncertainty. Across multiple datasets, task types, and model families, we showed that attention divergence is highly predictive of answer correctness and outperforms many existing baselines, while requiring negligible computational overhead.

Beyond performance, our analyses provide insight into where this uncertainty is located. We find that the proposed signal is concentrated in middle layers and at factual anchors such as named entities and numerical values.

Overall, our work suggests that internal attention dynamics contain reliable uncertainty signals that can be extracted with minimal computational cost. We believe that leveraging such white-box signals is a promising direction for improving the reliability and transparency of large language models.

8 Limitations

Despite the good results, there are a few important limitations to note.

First, while attention divergence is highly correlated with hallucinated and incorrect outputs, our work does not establish a causal relationship between specific patterns and false generations. The uncertainty signal is distributed across multiple heads and layers, and cannot be reduced to a simple logical rule such as "high divergence in a particular head implies an incorrect answer". As a result, our findings should be interpreted as a predictive signal.

Secondly, although the lasso regularized probe identifies informative attention heads, the resulting model remains difficult to interpret. Consequently, the probe should not be viewed as an explanation of how uncertainty is represented, but rather as a tool for extracting the signal. Future research could try to set up a method that does not use any probe at all, by finding a relation as to which heads are predictive of hallucinations or answer correctness.

Our model requires access to internal model architecture, with attention weights in particular, and therefore cannot be applied to black-box models that only give the generated text or output probabilities. However, this highlights the value of open and transparent model architectures.

Although attention divergence itself is an informative signal, the specific combination of heads and layers selected by the probe varies across datasets and families. This suggests that a logistic regression probe might be too specific for uncertainty quantification.

References

- Alexandra Bazarova, Aleksandr Yugay, Andrey Shulga, Alina Ermilova, Andrei Volodichev, Konstantin Polev, Julia Belikova, Rauf Parchiev, Dmitry Simakov, Maxim Savchenko, Andrey Savchenko, Serguei Barannikov, and Alexey Zaytsev. 2025. [Hallucination Detection in LLMs with Topological Divergence on Attention Graphs](#).
- Jakub Binkowski, Denis Janiak, Albert Sawczyn, Bogdan Gabrys, and Tomasz Kajdanowicz. 2025. [Hallucination detection in LLMs using spectral features of attention maps](#).
- Sky CH-Wang, Benjamin Van Durme, Jason Eisner, and Chris Kedzie. 2024. [Do androids know they're only dreaming of electric sheep?](#) In *Findings of the Association for Computational Linguistics: ACL 2024*, pages 4401–4420, Bangkok, Thailand. Association for Computational Linguistics.
- Chao Chen, Kai Liu, Ze Chen, Yi Gu, Yue Wu, Mingyuan Tao, Zhihang Fu, and Jieping Ye. 2024. [INSIDE: LLMs' internal states retain the power of hallucination detection](#).
- Yung-Sung Chuang, Linlu Qiu, Cheng-Yu Hsieh, Ranjay Krishna, Yoon Kim, and James Glass. 2024. [Lookback Lens: Detecting and mitigating contextual hallucinations in large language models using only attention maps](#).
- Karl Cobbe, Vineet Kosaraju, Mohammad Bavarian, Mark Chen, Heewoo Jun, Lukasz Kaiser, Matthias Plappert, Jerry Tworek, Jacob Hilton, Reiichiro Nakano, Christopher Hesse, and John Schulman. 2021. Training verifiers to solve math word problems. *arXiv preprint arXiv:2110.14168*.
- Xuefeng Du, Chaowei Xiao, and Yixuan Li. 2024. [HaloScope: Harnessing Unlabeled LLM Generations for Hallucination Detection](#).
- Nelson Elhage, Neel Nanda, Catherine Olsson, Tom Henighan, Nicholas Joseph, Ben Mann, Amanda Askell, Yuntao Bai, Anna Chen, Tom Conerly, Nova DasSarma, Dawn Drain, Deep Ganguli, Zac Hatfield-Dodds, Danny Hernandez, Andy Jones, Jackson Kernion, Liane Lovitt, Kamal Ndousse, and 6 others. 2021. A mathematical framework for transformer circuits. *Transformer Circuits Thread*. <https://transformer-circuits.pub/2021/framework/index.html>.
- Ekaterina Fadeeva, Aleksandr Rubashevskii, Artem Shelmanov, Sergey Petrakov, Haonan Li, Hamdy Mubarak, Evgenii Tsymbalov, Gleb Kuzmin, Alexander Panchenko, Timothy Baldwin, Preslav Nakov, and Maxim Panov. 2024. [Fact-Checking the output of large language models via Token-Level uncertainty quantification](#).
- Sebastian Farquhar, Jannik Kossen, Lorenz Kuhn, and Yarin Gal. 2024. [Detecting hallucinations in large language models using semantic entropy](#). *Nature*, 630(8017):625–630.
- Javier Ferrando, Oscar Obeso, Senthoran Rajamanoharan, and Neel Nanda. 2024. [Do I know this entity? Knowledge awareness and hallucinations in language models](#).
- Aaron Grattafiori, Abhimanyu Dubey, Abhinav Jauhri, Abhinav Pandey, Abhishek Kadian, and Al-Dahle. 2024. [The Llama 3 herd of models](#).
- Bairu Hou, Yujian Liu, Kaizhi Qian, Jacob Andreas, Shiyu Chang, and Yang Zhang. 2023. [Decomposing Uncertainty for Large Language Models through Input Clarification Ensembling](#).
- Lei Huang, Weijiang Yu, Weitao Ma, Weihong Zhong, Zhangyin Feng, Haotian Wang, Qianglong Chen, Weihua Peng, Xiaocheng Feng, Bing Qin, and Ting

- Liu. 2024. [A survey on hallucination in large language models: principles, taxonomy, challenges, and open questions](#). *ACM Transactions on Information Systems*, 43(2):1–55.
- Eyke Hüllermeier, Willem Waegeman, Eyke Hüllermeier, and Willem Waegeman. 2021. [Aleatoric and epistemic uncertainty in machine learning: an introduction to concepts and methods](#). *Machine Learning*, 110(3):457–506.
- Albert Q. Jiang, Alexandre Sablayrolles, Arthur Mensch, Chris Bamford, Devendra Singh Chaplot, Diego De Las Casas, Florian Bressand, Gianna Lengyel, Guillaume Lample, Lucile Saulnier, Léo Renard Lavaud, Marie-Anne Lachaux, Pierre Stock, Teven Le Scao, Thibaut Lavril, Thomas Wang, Timothée Lacroix, and William El Sayed. 2023. [Mistral 7B](#).
- Mandar Joshi, Eunsol Choi, Daniel S. Weld, and Luke Zettlemoyer. 2017. [TriviaQA: a large scale distantly supervised challenge dataset for reading Comprehension](#).
- Adam Tauman Kalai, Ofir Nachum, Santosh S. Vempala, and Edwin Zhang. 2025. [Why language models hallucinate](#).
- Yubin Kim, Hyewon Jeong, Shan Chen, Shuyue Stella Li, Chanwoo Park, Mingyu Lu, Kumail Alhamoud, Jimin Mun, Cristina Grau, Minseok Jung, Rodrigo Gameiro, Lizhou Fan, Eugene Park, Tristan Lin, Joonsik Yoon, Wonjin Yoon, Maarten Sap, Yulia Tsvetkov, Paul Liang, and 8 others. 2025. [Medical hallucinations in foundation models and their impact on healthcare](#).
- Armen Der Kiureghian and Ove Ditlevsen. 2009. [Aleatory or epistemic? does it matter?](#) *Structural Safety*, 31(2):105–112. Risk Acceptance and Risk Communication.
- Miroslav Kubat and Stan Matwin. 1997. [Addressing the curse of imbalanced training sets: One-sided selection](#). In *In Proceedings of the Fourteenth International Conference on Machine Learning*, pages 179–186. Morgan Kaufmann.
- Lorenz Kuhn, Yarin Gal, and Sebastian Farquhar. 2023. [Semantic uncertainty: Linguistic invariances for uncertainty estimation in natural language generation](#).
- Jing Li. 2024. [Area under the roc curve has the most consistent evaluation for binary classification](#). *Preprint*, arXiv:2408.10193.
- Yinghao Li, Rushi Qiang, Lama Moukheiber, and Chao Zhang. 2025. [Language Model Uncertainty Quantification with Attention Chain](#).
- Stephanie Lin, Jacob Hilton, and Owain Evans. 2021. [TruthfulQA: Measuring How models mimic Human Falsehoods](#).
- Chen Ling, Xujiang Zhao, Xuchao Zhang, Wei Cheng, Yanchi Liu, Yiyun Sun, Mika Oishi, Takao Osaki, Katsushi Matsuda, Jie Ji, Guangji Bai, Liang Zhao, and Haifeng Chen. 2024. [Uncertainty quantification for In-Context learning of large language models](#).
- Xiaou Liu, Tiejun Chen, Longchao Da, Chacha Chen, Zhen Lin, and Hua Wei. 2025. [Uncertainty quantification and confidence calibration in large language models: a survey](#).
- Varun Magesh, Faiz Surani, Matthew Dahl, Mirac Suzgun, Christopher D. Manning, and Daniel E. Ho. 2024. [Hallucination-Free? Assessing the reliability of leading AI legal research tools](#). *arXiv*.
- Potsawee Manakul, Adian Liusie, and Mark J. F. Gales. 2023. [SelfCheckGPT: Zero-Resource Black-Box Hallucination Detection for Generative Large Language Models](#).
- Yuya Ogasa and Yuki Arase. 2025. [Hallucinated Span Detection with Multi-View Attention Features](#).
- Hadas Orgad, Michael Toker, Zorik Gekhman, Roi Reichart, Idan Szpektor, Hadas Kotek, and Yonatan Belinkov. 2024. [LLMs know more than they show: on the intrinsic representation of LLM hallucinations](#).
- Maja Pavlovic. 2025. [Understanding Model Calibration – A gentle introduction and visual exploration of calibration and the expected calibration error \(ECE\)](#).
- Jie Ren, Jiaming Luo, Yao Zhao, Kundan Krishna, Mohammad Saleh, Balaji Lakshminarayanan, and Peter J. Liu. 2022. [Out-of-Distribution detection and selective generation for conditional language models](#).
- Gaurang Sriramanan, Siddhant Bharti, Vinu Sankar Sadasivan, Shoumik Saha, Priyatham Kattakinda, and Soheil Feizi. 2024. [Llm-check: Investigating detection of hallucinations in large language models](#). In *Advances in Neural Information Processing Systems*, volume 37, pages 34188–34216. Curran Associates, Inc.
- Alessandro Stolfo, Ben Wu, Wes Gurnee, Yonatan Belinkov, Xingyi Song, Mrinmaya Sachan, and Neel Nanda. 2024. [Confidence regulation neurons in language models](#).
- Zhongxiang Sun, Xiaoxue Zang, Kai Zheng, Yang Song, Jun Xu, Xiao Zhang, Weijie Yu, Yang Song, and Han Li. 2024. [REDEEP: Detecting Hallucination in Retrieval-Augmented Generation via Mechanistic Interpretability](#).
- Ashish Vaswani, Noam Shazeer, Niki Parmar, Jakob Uszkoreit, Llion Jones, Aidan N. Gomez, Lukasz Kaiser, and Illia Polosukhin. 2017. [Attention is all you need](#).
- Artem Vazhentsev, Lyudmila Rvanova, Gleb Kuzmin, Ekaterina Fadeeva, Ivan Lazichny, Alexander Panchenko, Maxim Panov, Timothy Baldwin, Mrinmaya Sachan, Preslav Nakov, and Artem Shelmanov.

2025. [Uncertainty-Aware Attention Heads: Efficient unsupervised uncertainty quantification for LLMs.](#)

Cheng Wang. 2023. [Calibration in Deep Learning: A Survey of the State-of-the-Art.](#)

An Yang, Anfeng Li, Baosong Yang, Beichen Zhang, Binyuan Hui, Bo Zheng, Bowen Yu, Chang Gao, Chengen Huang, Chenxu Lv, Chujie Zheng, Dayiheng Liu, Fan Zhou, Fei Huang, Feng Hu, Hao Ge, Haoran Wei, Huan Lin, Jialong Tang, and 41 others. 2025. [QWEN3 Technical Report.](#)

Zhilin Yang, Peng Qi, Saizheng Zhang, Yoshua Bengio, William W. Cohen, Ruslan Salakhutdinov, and Christopher D. Manning. 2018. [HotpotQA: a dataset for diverse, explainable multi-hop question answering.](#)

Shengyu Zhang, Linfeng Dong, Xiaoya Li, Sen Zhang, Xiaofei Sun, Shuhe Wang, Jiwei Li, Runyi Hu, Tianwei Zhang, Fei Wu, and Guoyin Wang. 2023. [Instruction tuning for large language models: A survey.](#)

Wayne Xin Zhao, Kun Zhou, Junyi Li, Tianyi Tang, Xiaolei Wang, Yupeng Hou, Yingqian Min, Beichen Zhang, Junjie Zhang, Zican Dong, Yifan Du, Chen Yang, Yushuo Chen, Zhipeng Chen, Jinhao Jiang, Ruiyang Ren, Yifan Li, Xinyu Tang, Zikang Liu, and 3 others. 2023. [A survey of large language models.](#)

Zifan Zheng, Yezhaohui Wang, Yuxin Huang, Shichao Song, Bo Tang, Feiyu Xiong, and Zhiyu Li. 2024. [Attention heads of large language models: A survey.](#) *ArXiv*, abs/2409.03752.

A Appendix

A.1 Experimental Setup

A.1.1 Attention Extraction

During greedy decoding, we extract attention weights on the full sequence (prompt plus generated tokens) with `output_attentions=True` and `use_cache=True`. We use the model’s returned post-softmax self-attention matrices for each generated token.

For each generated token t , and for each attention head h in layer l we obtain the attention distribution over all positions $\{1, \dots, t-1\}$. We measure how concentrated this is by computing its Kullback–Leibler (KL) divergence to a uniform distribution over the same $t+1$ positions. KL divergence is computed using natural logarithms, with a small ϵ value to clamp results for stability.

For each head, the divergence values are averages over all generated token positions, resulting in a single scalar per head. Finally, all head features are concatenated into a feature vector $x \in \mathbb{R}^{L \times H}$, where L is the number of layers and H the number of heads per layer.

A.1.2 TruthfulQA Answers

For each example we use the MC1 (Multiple-choice 1) choice set from `mc1_targets`. We randomly permute the choices per example, and define the correct answer as the index where the permuted labels equals 1. Since in the base dataset the correct answer is always the first one. The model is prompted to output a single letter (A, B, C, ...) (see Table 8). We extract the predicted letter and map it back to an index. Predictions without a letter are marked as incorrect.

A.2 Directions for Future Research

There are several interesting directions for future research building on our measure. First, while our results show that uncertainty lives strongest in the middle layers and is distributed across multiple heads, the underlying mechanisms remain unclear. Future work could focus on identifying groups of heads and layers that together encode uncertainty. Attention heads could be clustered based on similarity in their behaviour. Secondly, the current probing approach relies on linear logistic regression with lasso regularization. While this works great for selecting a sparse subset of heads, future work could explore alternative probing methods that capture richer structure.

Additionally, training probes on one dataset and evaluating them on others would allow for a better assessment on how uncertainty generalizes. Our token analysis indicates that attention divergence is mainly concentrated on semantically meaningful tokens, such as named entities, numbers, and dates. This suggests the possibility of localizing hallucinations within a generation rather than just scoring entire answers. Future work could try to compute attention divergence autoregressively to identify when a hallucination happens. This could allow models to highlight or flag specific parts of an output that are likely to be unreliable. Additionally, by comparing generations produced with and without retrieval augmented context (RAG), it would be possible to test whether divergence decreases when reliable external evidence is provided. Another direction for future research is evaluating attention divergence on a broader range of datasets and tasks types. In this paper, we mainly focus on question answering and reasoning, where correctness is easy to define. For instance, we did not include experiments for machine translation tasks due to the difficulty of defining and anno-

tating hallucinations or factual errors in generated translations.

Finally, attention divergence could potentially be used not only as a diagnostic signal (detecting hallucinations), but also as a training objective. A promising direction is to use reinforcement learning or other fine tuning approaches that penalize extreme attention divergence at critical tokens, such as named entities or numerical values. This may encourage the model to reduce hallucinations while still being fluent

A.3 Data

A.3.1 Full Main Results

Table 7 shows the full results of our experiment, including Expected Calibration Error (ECE) and accuracy along AUROC.

A.3.2 Sanity Check

As said in section 5.3 we performed several sanity checks to see whether our measure could be influenced by other factors, such as generation length. The results can be found below in table 6.

Baseline	AUROC
Generation length	0.36
Prompt length	0.44
Raw output length	0.37
Ends with punctuation	0.54
Number of digits	0.48
Generation length (perm.)	0.50

Table 6: AUROC of sanity check features on TriviaQA using Llama-3.2-3B-Instruct. All baselines are evaluated independently using a single random seed. Permutation results are included as a sanity check.

Dataset	Model	AUROC	Accuracy	ECE
TruthfulQA	Llama-3.2-3B-Instruct	0.906 \pm 0.024	0.838 \pm 0.029	0.201 \pm 0.012
	Qwen3-4B-Instruct	0.906 \pm 0.025	0.827 \pm 0.026	0.224 \pm 0.010
	Mistral-7B-Instruct-v0.2	0.891 \pm 0.024	0.801 \pm 0.029	0.219 \pm 0.017
TriviaQA	Llama-3.2-3B-Instruct	0.835 \pm 0.004	0.791 \pm 0.002	0.059 \pm 0.005
	Qwen3-4B-Instruct	0.846 \pm 0.001	0.770 \pm 0.005	0.064 \pm 0.001
	Mistral-7B-Instruct-v0.2	0.835 \pm 0.004	0.791 \pm 0.002	0.059 \pm 0.005
HotpotQA	Llama-3.2-3B-Instruct	0.8035 \pm 0.0219	0.7648 \pm 0.0140	0.0644 \pm 0.0155
	Qwen3-4B-Instruct	0.7963 \pm 0.0217	0.7957 \pm 0.0225	0.0862 \pm 0.0050
	Mistral-7B-Instruct-v0.2	0.7782 \pm 0.0061	0.7613 \pm 0.0078	0.0957 \pm 0.0071
GSM8K	Llama-3.2-3B-Instruct	0.7672 \pm 0.0305	0.7692 \pm 0.0137	0.0601 \pm 0.0177
	Qwen3-4B-Instruct	0.9450 \pm 0.0151	0.9166 \pm 0.0132	0.0501 \pm 0.0078
	Mistral-7B-Instruct-v0.2	0.7889 \pm 0.0270	0.7301 \pm 0.0129	0.0439 \pm 0.0146

Table 7: Results on validation set after training a lasso regularization probe to predict correctness from attention divergence mean pooled across the whole generation. Within each dataset, the highest AUROC and accuracy and the lowest ECE are shown in bold. Results are reported as mean \pm standard deviation over three random seeds and 5 stratified cross-validation folds.

Parameter	Value
<i>Models and evaluation</i>	
Models	Llama-3.2-3B-Instruct, Mistral-7B-Instruct-v0.2, Qwen3-4B-Instruct-2507
ECE bins	10
<i>Probe and training</i>	
Probe	Logistic regression (L1 / lasso)
Solver	saga
Regularization strength (C)	1.0
Max probe iterations	20,000
Train / validation split	80% / 20% (stratified)
Cross-validation	5-fold stratified
Random seeds	3
<i>Generation and attention features</i>	
Decoding	Greedy ($T = 0$, no sampling)
Max new tokens	32 (HotpotQA, TriviaQA), 8 (TruthfulQA), 256 (GSM8K)
Attention aggregation	Mean over generated tokens
<i>Datasets</i>	
GSM8K	1319 samples; numeric answer extraction
TriviaQA	2000 samples; substring match against aliases
HotpotQA	2000 samples; context truncated to 2048 tokens
TruthfulQA	272 samples per seed; MC1 with shuffled choices
<i>Prompt per Dataset</i>	
GSM8K	<i>Solve the problem and give the final numeric answer.</i>
TriviaQA	<i>Answer the question briefly.</i>
HotpotQA	<i>Answer using the context. Be brief.</i>
TruthfulQA	<i>Answer with ONLY the letter (A, B, C, ...).</i>

Table 8: Experimental setup and hyperparameters. All settings apply to Llama, Mistral, and Qwen unless otherwise stated.

Model	Layer	Head	GSM8K	TruthfulQA	TriviaQA	HotpotQA	Total
Llama	21	02	10	–	–	6	16
	13	18	–	10	9	–	19
	17	06	9	–	–	–	9
	21	13	9	–	–	–	9
	10	10	–	10	–	–	10
	12	06	–	9	–	–	9
	13	21	–	9	–	–	9
	14	06	–	9	–	–	9
	14	10	–	9	–	–	9
	15	22	–	9	–	–	9
	23	15	–	9	–	–	9
	25	01	–	9	–	–	9

Continued on next page

Model	Layer	Head	GSM8K	TruthfulQA	TriviaQA	HotpotQA	Total
	03	09	8	–	–	–	8
	04	05	8	–	–	–	8
	20	08	8	–	–	–	8
	07	18	8	–	–	–	8
	21	05	–	–	–	8	8
	08	13	–	–	–	7	7
	08	22	–	–	–	7	7
	09	19	–	–	–	7	7
	18	09	–	–	–	7	7
	06	21	7	–	–	–	7
	16	09	7	–	–	–	7
	19	20	7	–	–	–	7
	24	12	7	–	–	–	7
	04	17	7	–	–	–	7
	18	12	–	–	–	6	6
	08	00	–	–	–	6	6
	14	13	–	–	–	6	6
	27	05	–	–	–	6	6
	08	14	–	–	6	6	12
	12	01	–	–	–	6	6
Qwen	22	02	–	10	–	–	10
	26	05	–	10	–	–	10
	22	00	–	9	–	–	9
	28	15	–	8	–	–	8
	31	08	–	8	–	–	8
	20	04	–	6	–	8	14
	25	05	–	–	–	8	8
	22	08	–	–	–	7	7
	23	12	–	–	–	7	7
	25	08	–	–	–	7	7
	30	10	–	–	6	–	6
	14	05	–	–	6	–	6
	00	13	–	6	–	–	6
	23	05	–	6	–	–	6
	27	05	–	6	–	–	6
	28	07	–	6	–	–	6
	30	00	–	6	–	–	6
	29	11	–	6	–	–	6
	00	01	4	–	–	5	9
	00	12	4	–	–	–	4
Mistral	31	02	10	–	6	8	24
	14	08	–	10	–	7	17
	14	10	–	10	–	–	10
	31	03	–	6	10	–	16
	10	23	–	9	–	–	9
	15	18	–	9	–	–	9
	16	20	–	9	–	–	9
	16	29	–	9	–	–	9

Continued on next page

Model	Layer	Head	GSM8K	TruthfulQA	TriviaQA	HotpotQA	Total
	30	07	7	–	–	–	7
	01	30	7	–	–	–	7
	06	19	7	–	–	–	7
	11	22	–	–	–	7	7
	21	04	–	–	–	7	7
	18	24	–	–	–	7	7
	05	26	–	–	–	6	6
	07	18	–	–	–	6	6
	12	17	–	–	–	6	6
	16	01	–	–	–	6	6
	18	23	–	–	6	6	12

Table 9: All attention heads selected by the L1 probe across models, datasets, and random seeds. Values denote the number of seeds (out of 10) in which a head was selected. A dash (–) indicates that the head was not selected for that dataset.